

See discussions, stats, and author profiles for this publication at: <https://www.researchgate.net/publication/224050926>

# Potential Role of a Quetiapine Metabolite in Quetiapine-Induced Neutropenia and Agranulocytosis

ARTICLE *in* CHEMICAL RESEARCH IN TOXICOLOGY · APRIL 2012

Impact Factor: 3.53 · DOI: 10.1021/tx2005635 · Source: PubMed

---

CITATIONS

13

---

READS

47

## 2 AUTHORS:



Xiaohai Li

The Scripps Research Institute

14 PUBLICATIONS 520 CITATIONS

SEE PROFILE



Michael D Cameron

The Scripps Research Institute

102 PUBLICATIONS 2,372 CITATIONS

SEE PROFILE

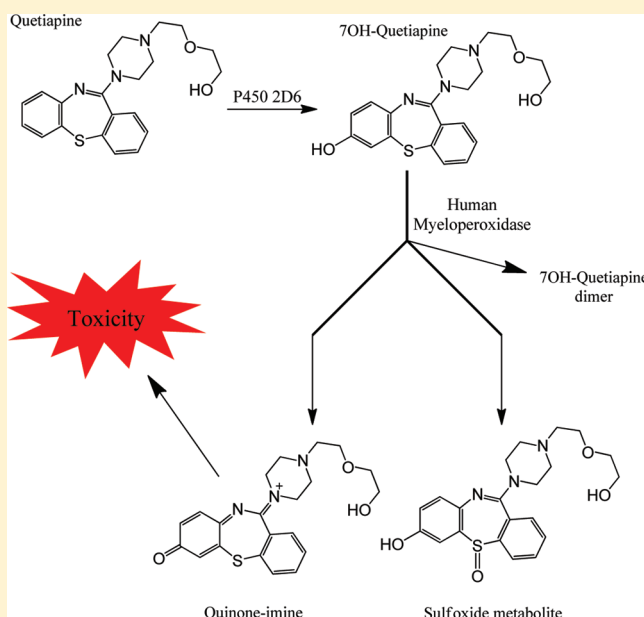
## Potential Role of a Quetiapine Metabolite in Quetiapine-Induced Neutropenia and Agranulocytosis

Xiaohai Li and Michael D. Cameron\*

Department of Molecular Therapeutics, The Scripps Research Institute, Scripps Florida, 130 Scripps Way, Jupiter, Florida 33458, United States

## S Supporting Information

**ABSTRACT:** Clozapine was the first of the atypical antipsychotics to be developed, but its use has been restricted because of toxicity issues, particularly the risk of potentially life-threatening drug-induced neutropenia and agranulocytosis, which occurs in about 1% of patients. Bioactivation of clozapine by peroxidases forms a reactive nitrenium ion, which covalently adducts to protein and leads to neutrophil toxicity. The current generation of clozapine-inspired atypical antipsychotics has reduced toxicity through improved potency/decreased dose or through structural modification to prevent peroxidase-catalyzed nitrenium ion formation. Through the substitution of sulfur for the bridging nitrogen found in clozapine, quetiapine does not directly form a nitrenium ion when incubated with myeloperoxidase/H<sub>2</sub>O<sub>2</sub>. We present evidence that cytochrome P450 2D6 catalyzes the formation of 7-hydroxyquetiapine, which can be oxidized by human myeloperoxidase to form a reactive quinone-imine and a reactive radical, which may account for the continued, although reduced, neutrophil toxicity. In the presence of myeloperoxidase/H<sub>2</sub>O<sub>2</sub> and glutathione, covalent 7-hydroxyquetiapine-glutathione adducts were formed. Bioactivation of quetiapine was verified in vivo in rat where three 7-hydroxyquetiapine-mercaptate adducts and a 7-hydroxyquetiapine-glutathione adduct were detected from bile after oral dosing. The decreased incidence of agranulocytosis with quetiapine over clozapine is postulated to be due to the lower exposure of the toxic precursor, 7-hydroxyquetiapine versus clozapine, respectively.



## ■ INTRODUCTION

Quetiapine (QTP) is one of several clozapine (CLZ)-inspired atypical antipsychotic drugs that were brought to the clinic for the treatment of schizophrenia<sup>1,2</sup> and acute manic episodes associated with bipolar disorder in adult patients.<sup>3,4</sup> CLZ has been demonstrated to be metabolized by human peroxidases to form a reactive metabolite that covalently binds to cellular proteins.<sup>5,6</sup> Because of the high peroxidase activity in neutrophils, CLZ is particularly toxic to white blood cells, and the incidence of severe decreases in cell count, agranulocytosis, is approximately 1 in 100 patients.<sup>7</sup> For this reason, routine blood tests are required for patients taking CLZ.

Second and third generation CLZ-inspired atypical antipsychotics have superior safety profiles accomplished primarily through increases in potency, which allow for decreased dose or through structural modification to decrease reactive metabolite formation. QTP is dosed at comparable levels to CLZ but has been structurally modified to replace the bridging nitrogen with a sulfur to prevent bioactivation to a reactive nitrenium ion

catalyzed by peroxidases (Figure 1).<sup>5,8</sup> While the safety profile of QTP is improved, it is still associated with reduction in white blood cell count, which leads to infrequent adverse effects including leucopenia and thrombocytopenia.<sup>9–12</sup> Additionally, QTP treatment is also associated with common asymptomatic increases of liver enzymes (retrospective chart review of 312 patients found greater than the normal ranges in one or more liver enzymes in 27.1% of QTP-treated patients).<sup>13</sup> While most cases are asymptomatic, incidences of fatal hepatotoxicity stemming from clinical use of QTP have been reported.<sup>14–16</sup>

The primary clearance of QTP is through hepatic metabolism, predominantly by P450 3A4/5 and to a lesser extent by P450 2D6. QTP undergoes a complex metabolic fate, which results in approximately 20 metabolites including sulfoxidation, hydroxylation of the dibenzothiazepine ring, N-

Received: December 30, 2011

Published: April 16, 2012



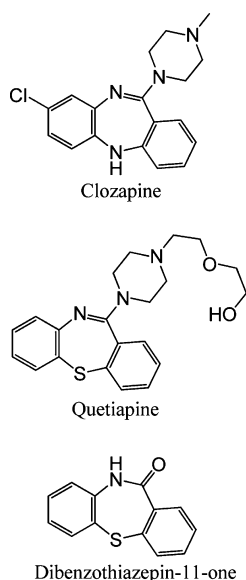


Figure 1. Molecular structures.

and O-dealkylation, and oxidation of the alkyl side chain to a carboxylic acid.<sup>17–19</sup>

In this study, the bioactivation of QTP and its metabolite 7-hydroxyquetiapine (7OH-QTP) was investigated in vitro. The formation of GSH adducts of QTP in GSH- and NADPH-fortified human liver microsomal incubations was detected. Bioactivation of QTP and 7OH-QTP by myeloperoxidases (MPO) and horseradish peroxidase (HRP) in GSH and potassium cyanide-trapping experiments is reported. Additionally, the generated glutathione adduct was demonstrated to be formed in vivo after oral dosing of QTP in rat. Our results confirmed the generation of an electrophilic reactive metabolite by QTP and established for the first time a possible link between the clinically observed neutropenia and hepatotoxicity and the 7-hydroxy metabolite. Furthermore, given the role of the polymorphically expressed enzyme P450 2D6 in the formation of 7OH-QTP, it would be of great interest to see if P450 2D6 null, normal, and ultrarapid metabolizers would generate differing concentrations of 7OH-QTP and alter individual susceptibility to QTP-induced neutropenia.

## EXPERIMENTAL PROCEDURES

**Chemicals and Reagents.** All reagents and solvents were either analytical or HPLC grade. QTP and 7OH-QTP (>99% purity) were purchased from LC Laboratories (Woburn, MA). HRP type VI (256 U/mg protein), H<sub>2</sub>O<sub>2</sub> (35% w/v in H<sub>2</sub>O), L-ascorbic acid, ketoconazole, quinidine, dextrophan, CLZ, N-acetyltyrosine (NAT), glutathione (reduced form, GSH), and potassium cyanide were purchased from Sigma-Aldrich (St. Louis, MO). K<sup>13</sup>C<sup>15</sup>N (>99% <sup>13</sup>C, >98% <sup>15</sup>N) was purchased from Cambridge Isotopes. Human MPO was from RnD Systems (Minneapolis, MN). Pooled 150 donor human liver microsomes and recombinant P450s (EasyCYP bacosomes, prepared from *Escherichia coli* coexpressing recombinant human NADPH-P450 reductase) were purchased from XenoTech LLC (Lenexa, KS). Formic acid, dimethyl sulfoxide (DMSO), and acetonitrile were purchased from Fisher Scientific (Fair Lawn, NJ).

**In Vitro Metabolism and Trapping Experiments.** Pooled mixed gender human donor microsomes and recombinant P450 (EasyCYP bacosomes) were thawed on ice. QTP or 7OH-QTP (20 μM) was incubated separately in reactions containing 100 mM potassium phosphate buffer (pH 7.4) and 1 mM NADPH in a final volume of 0.5 mL. The human liver microsome (HLM) protein concentration is noted in the figure legends. Recombinant P450

incubations with QTP or 7OH-QTP were performed similarly except that HLMs were replaced by EasyCYP bacosomes (50 pmol/mL). Control experiments without substrate or NADPH were included. Trapping experiments contained 5 mM reduced glutathione or 4 mM potassium cyanide of a 1:1 ratio of KCN/K<sup>13</sup>C<sup>15</sup>N. All incubations were performed at 37 °C in a shaking incubator. Reactions were stopped by the addition of 500 μL of CH<sub>3</sub>CN (with or without addition of 0.1 μM dextrophan as an analytical internal standard). Samples were mixed on a vortex mixer and centrifuged at 10000g for 10 min at 4 °C to pellet proteins, and supernatants were dried down in a vacuum centrifuge. The dried samples were reconstituted in 100 μL of 30% CH<sub>3</sub>CN.

**In Vitro Peroxidase Experiments.** QTP, 7OH-QTP, and CLZ (20 μM) were, respectively, incubated at 37 °C with peroxidase (the final concentrations were 2 μg/mL MPO or 20 U/mL HRP), 0.4 M KCl, and 0.8 mM H<sub>2</sub>O<sub>2</sub> in phosphate buffer (100 μM, pH 7.4). The final incubation volume was 0.25 mL. The reaction was terminated by adding ascorbic acid (2 mM final) and CH<sub>3</sub>CN. Trapping experiments were performed as described above with the addition of control samples lacking peroxidase or H<sub>2</sub>O<sub>2</sub>.

### LC-MS/MS Analysis of Glutathione and Cyanide Adducts.

LC-UV-MS/MS analysis was performed using an API 4000 Q-Trap mass spectrometer interfaced with an Agilent 1200 HPLC with a diode array detector. Glutathione adducts were detected through a negative precursor ion (PI) scan of *m/z* 272, corresponding to GSH fragmenting at the thioether bond. This triggered positive ion enhanced resolution and enhanced product ion scans. Cyanide adducts were detected using two neutral loss (–27/–29 AMU) triggered enhanced product ion scans, and results were validated by the presence of the isotope pattern (1:1 ratio with a mass difference of 2 AMU), which was afforded by using 1:1 KCN/K<sup>13</sup>C<sup>15</sup>N as the trapping agent. Chromatographic separations were performed on an Agilent Eclipse XDB C18 column (3.5 μm, 3.0 mm × 150 mm) run at 400 μL/min with linear gradient elution (mobile phase A = 0.1% v/v formic acid in water, mobile phase B = acetonitrile with 0.1% v/v formic acid), 0–3 min = 5% B, 3.5 min = 10% B, 23 min = 50% B, 28 = 80% B, 30 min = 80% B, 30.5 min = 5% B, and 36 min = 5% B. Any potential adducts were initially characterized by comparing incubated samples to control samples without NADPH, glutathione, KCN/K<sup>13</sup>C<sup>15</sup>N, or substrate.

**MPO-Catalyzed 7OH-QTP Dimer Formation.** In the absence of trapping agents, MPO catalyzed the formation of a 7OH-QTP dimer. Incubation conditions were the same as those given in the Peroxidase Incubations section. A mass range of 600–800 AMU was scanned with triggered enhanced product ion scans. To test if dimer formation was due to the combination of radicals, dimer formation was evaluated in the presence and absence of NAT, which is oxidized to a free radical by MPO.<sup>20</sup> The NAT concentration was varied between 100 μM and 4 mM.

**Bioactivation in Rat.** The bile duct was cannulated in three male Sprague–Dawley rats according to standard procedures as approved by the Scripps Florida IACUC. Rats were allowed to recover from surgery for 2 days, and on day three, bile samples were collected immediately prior to giving an oral dose of QTP by gavage (20 mg/kg). Additional bile samples were collected 2 and 7 h postdose. Samples were processed by two methods: through direct injection of the soluble fraction after adding an equal volume of CH<sub>3</sub>CN and centrifugation or by an extraction method where an equal volume of CH<sub>3</sub>CN was added followed by the addition of excess solid sodium chloride to make a saturated brine solution, which caused the aqueous and CH<sub>3</sub>CN fractions to separate into distinct layers. Subsequently, the CH<sub>3</sub>CN layer was analyzed. All samples were evaluated by LC-MS/MS using targeted multiple reaction monitoring (MRM) and total ion scans designed to detect QTP, 7OH-QTP, and corresponding GSH and mercapturic acid (N-acetyl cysteine) adducts. Samples simply treated with an equal volume of CH<sub>3</sub>CN had increased noise and background upon LC-MS/MS analysis but allowed for detection of a glutathione adduct, which was not observed using the extraction method.

## RESULTS

**Formation of QTP-GSH Adducts in HLMs and Recombinant P450s.** Incubation of QTP with HLMs in the presence of GSH resulted in the formation of at least four distinct GSH adducts (Figure 2A). Three of the GSH adducts

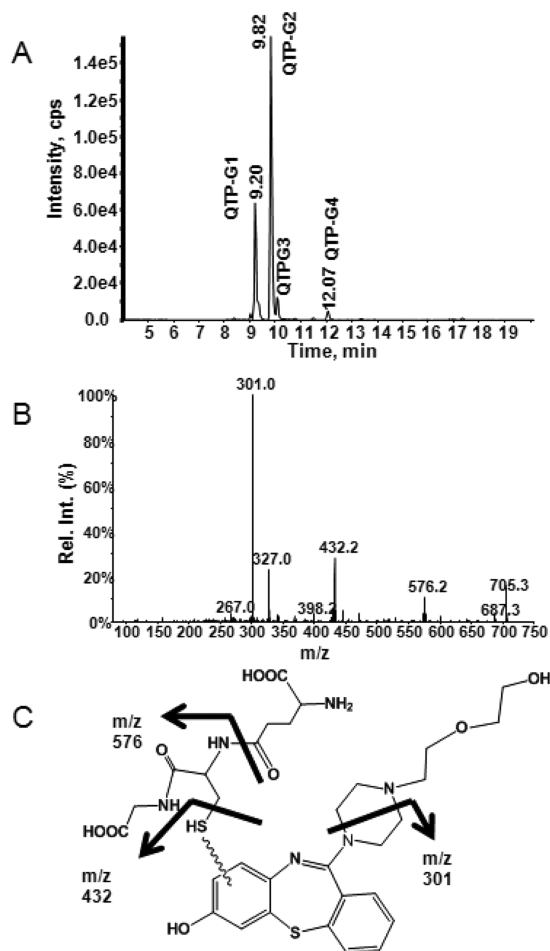


**Figure 2.** Formation of 7OH-QTP-GSH adducts in HLM incubations. Panel A represents the extracted ion chromatogram ( $m/z$  617 and 705) for detected glutathione adducts from a 60 min HLM incubation containing 2 mg of HLM protein/mL, 20  $\mu$ M QTP, 1 mM NADPH, and 5 mM GSH. The MS/MS spectrum from the 9.82 min peak is shown in B, and the proposed fragmentation pattern is provided in C. The spectra of the other adducts are provided in the Supporting Information.

had molecular ions of  $m/z$  705 and corresponded to the addition of one oxygen and GSH. The fourth (QTP-G1) was a secondary metabolite corresponding to the addition of oxygen and GSH to N-dealkylated QTP. The MS/MS spectrum and proposed fragmentation ions are given in Figure 2B,C (MS/MS spectra for all peaks are provided in the Supporting Information). A known human metabolite of QTP is 7OH-QTP, which is available from commercial sources. When the incubation was repeated with 7OH-QTP in place of QTP, GSH adducts with identical retention times and MS/MS fragmentation patterns as shown in Figure 2A were detected with the only difference being a slight decrease in the relative concentration of the dealkylated metabolite QTP-G1 (Supporting Information).

To determine the contribution of individual P450 enzymes in the formation of QTP-GSH adducts and the importance of the 7OH-QTP metabolite, cDNA-expressed human P450 enzymes (1A1, 1A2, 2B6, 2C8, 2C9, 2C19, 2D6, 3A4, and 3A5) were utilized. The highest concentration of glutathione adducts was detected in incubations containing P450 2D6 (Figure 3A). The

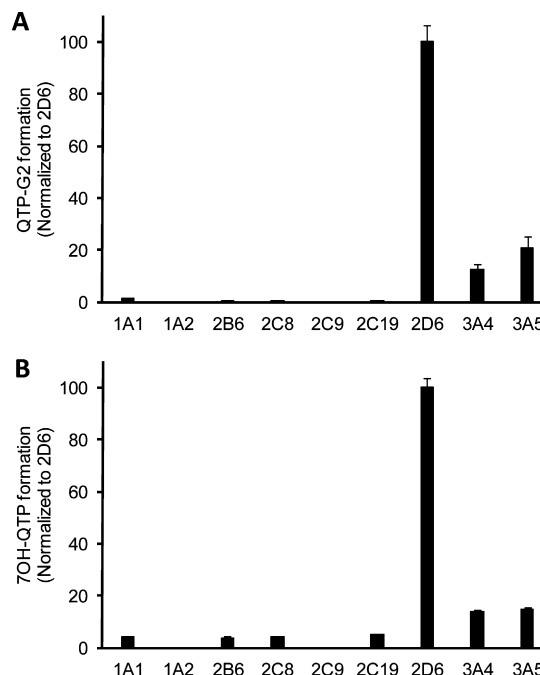


**Figure 3.** Generation of 7OH-QTP-GSH and 7OH-QTP by recombinant P450. Glutathione adducts corresponding to QTP + oxygen + GSH ( $m/z$  = 705 AMU) were detected in incubations containing 20  $\mu$ M QTP, 5 mM GSH, 1 mM NADPH, and 50 pmol/mL recombinant P450 (A). This was compared to the formation of 7OH-QTP in parallel incubations that did not contain GSH (B). Data are the average of duplicate incubations. In both graphs, the detected peak areas were normalized to P450 2D6.

detected adducts were the same as those seen in HLM reactions (Figure 2A) with the only difference being the minimal amounts of the dealkylated adduct. The production of 7OH-QTP was measured in parallel incubations that did not contain glutathione. The relative concentration of 7OH-QTP, as determined by LC-MS/MS peak area, was at least 7 times higher in P450 2D6 incubations than with other P450s (Figure 3B). When 7OH-QTP was used as the substrate instead of QTP, several P450 enzymes were capable of catalyzing the formation of glutathione conjugates (Supporting Information).

The generation of 7OH-QTP in incubations containing 20  $\mu$ M QTP and 0.1 mg of HLM microsomal protein/mL was evaluated with selective chemical inhibitors of P450 2D6 and 3A4/5. The addition of 10  $\mu$ M of the P450 2D6 inhibitor quinidine decreased 7OH-QTP formation by  $59 \pm 4\%$ , whereas the addition of 1  $\mu$ M P450 3A4/5 inhibitor ketoconazole decreased 7OH-QTP formation by  $37 \pm 8\%$  (Figure 4). When both inhibitors were present, 7OH-QTP formation was inhibited by  $93 \pm 1\%$ . Similar data were observed for QTP-G2, the largest 7OH-QTP-GSH peak, when glutathione was added to the incubations.

**Formation of Cyanide Adducts in HLMs.** The formation of cyanide adducts in incubations of CLZ, QTP, and 7OH-QTP was evaluated in HLM incubations. Cyanide adducts were



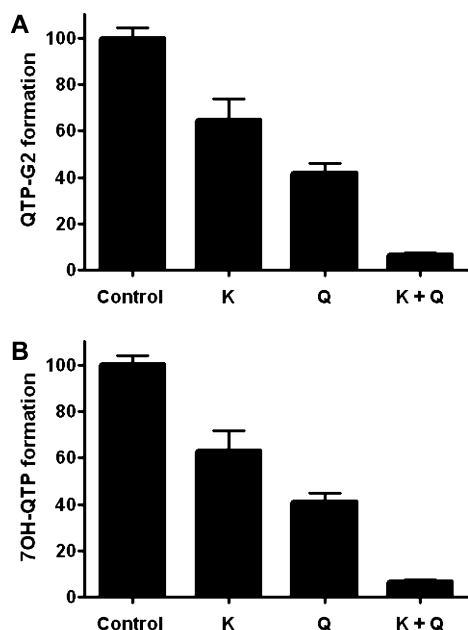


**Figure 4.** Inhibition of QTP-G2 and 7OH-QTP formation. The effect of ketoconazole (1  $\mu$ M), quinidine (10  $\mu$ M), or both inhibitors in the formation of QTP-G2 and 7OH-QTP was tested. Incubations ( $n = 3$ ) contained 20  $\mu$ M QTP and 1 mM NADPH with or without 5 mM GSH. Incubations measuring QTP-G2 formation were 30 min with 1 mg of HLM protein/mL, and incubations measuring 7OH-QTP formation were 15 min with 0.1 mg of HLM protein/mL. The relative amount of QTP-G2 (A) and 7OH-QTP (B) formed was referenced to the solvent control samples.

detected for all of the compounds by LC-MS/MS with CLZ-CN  $m/z = 352$ , QTP-CN  $m/z = 409$ , and 7OH-QTP  $m/z = 425$ . The abundance of the cyanide adducts in HLM incubations was low and undetectable by LC-UV even with high drug concentration or extended incubation periods.

**MPO-Catalyzed Bioactivation.** The bioactivation of QTP was compared to the more thoroughly studied analogue CLZ. Incubation of CLZ with MPO has been shown by other researchers to form a reactive metabolite that covalently adducts to cellular proteins.<sup>5,6</sup> In our hands, GSH trapping experiments with MPO worked well, but cyanide trapping experiments were complicated because cyanide is a potent inhibitor of MPO and because MPO oxidizes cyanide to form the cyanyl radical.<sup>21,22</sup> MPO experiments were repeated with HRP, which had fewer complications due to the formation of cyanyl radical. Both data sets are presented.

The stability of CLZ, QTP, and 7OH-QTP was evaluated in MPO incubations (Figure 5). CLZ levels were minimally depleted in MPO incubations containing  $H_2O_2$ , but oxidative metabolites with +16 and +18 AMU were detected. The extent of CLZ depletion was not significantly changed when GSH was added to the incubation, but the above-mentioned metabolites were replaced by two major GSH adducts with  $m/z = 632$  AMU, corresponding to the direct conjugation of GSH to CLZ. One major and two minor cyanide adducts were detected, all having  $m/z = 352$  AMU. QTP concentrations were not decreased in MPO incubations. QTP-GSH adducts were not detected, but two cyanide adducts with  $m/z = 409$  AMU were. These were produced in minimal yield and could not be detected by LC-UV. Depletion of 7OH-QTP in the absence of trapping agents was primarily accounted for by formation of 7OH-QTP homodimer. When GSH was added to the

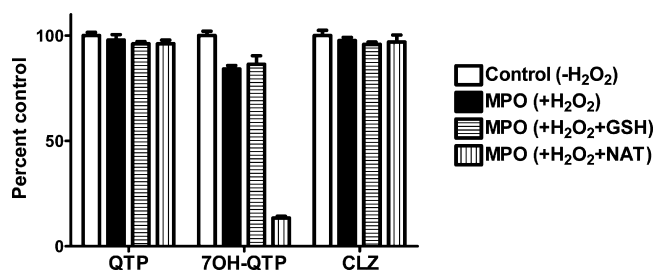


**Figure 5.** MPO-catalyzed compound depletion. The percent of parent drug (20  $\mu$ M QTP, 7OH-QTP, or CLZ) remaining after a 20 min incubation containing 2  $\mu$ g/mL MPO and 0.4 M KCl in 100  $\mu$ M phosphate buffer, pH 7.4. Incubations also contained 0.8 mM  $H_2O_2$ , 5 mM GSH, or 5 mM NAT as indicated. The percent remaining QTP, 7OH-QTP, or CLZ was determined by LC-MS/MS. Data are from triplicate samples and are normalized against the  $-H_2O_2$  control.

incubation, significant levels of GSH-7OH-QTP adducts were detected by LC-UV at 254 nm along with a corresponding decrease in the 7OH-QTP peak area. In the presence of cyanide, one major cyanide adduct was observed with  $m/z = 425$  AMU.

If trapping agents such as glutathione or cyanide were not added to the MPO reactions, 7OH-QTP formed a dimer with  $m/z = 797$  AMU. To evaluate if the dimerization proceeds through a free radical mechanism, we included NAT. When 7OH-QTP and NAT were coincubated with MPO and  $H_2O_2$ , multiple cross dimers of 7OH-QTP-NAT were detected with  $m/z = 621$  AMU, consistent with the 7OH-QTP dimer being formed through a free radical mechanism.<sup>20,23</sup>

**HRP-Catalyzed Bioactivation.** Whereas QTP and CLZ were minimally depleted in MPO incubations, large differences were observed with HRP. CLZ was oxidized to form a reactive species, which covalently adducted with either GSH or cyanide (Figure 6C). When evaluated using LC-UV, almost all of the CLZ was depleted, and new peaks corresponding to either the GSH or the cyanide adduct were detected, which appeared to be stoichiometric. QTP was not depleted, and adducts were not observed (Figure 6A). However, 7OH-QTP was efficiently metabolized by HRP. If the incubation was allowed to proceed for longer incubation times, diglutathione and triglutathione adducts of 7OH-QTP were detected (the small peak to the left of the labeled 7OH-QTP-GSH peaks in Figure 6B was identified as a di-GSH adduct by LC-MS/MS). The summation of the peak areas for the GSH adducts were greater than the original area of 7OH-QTP, which may be due to changes in the molar extinction coefficient at 254 nm for the adducts (Figure 6B). A major cyanide adduct of 7OH-QTP was observed with peak area that suggested nearly full conversion of 7OH-QTP to 7OH-QTP-CN.

**Dibenzothiazepin-11-one.** To strengthen the hypothesis that the quinone-imine was responsible for the detected glutathione adducts and not a nitrenium ion centered on the piperazine, dibenzothiazepin-11-one (a precursor in QTP synthesis, Figure 1) was evaluated. When incubated with HLM, cyanide adducts were not observed, but at least two monohydroxylated GSH adducts were detected (see the Supporting Information). No adducts or dimers were detected when directly incubated with MPO; however, when the major hydroxy-dibenzothiazepin-11-one metabolite generated in HLM incubations was isolated by solid-phase extraction, MPO rapidly oxidized it to form a reactive metabolite, which was able to be trapped with glutathione. Cyanide adducts were

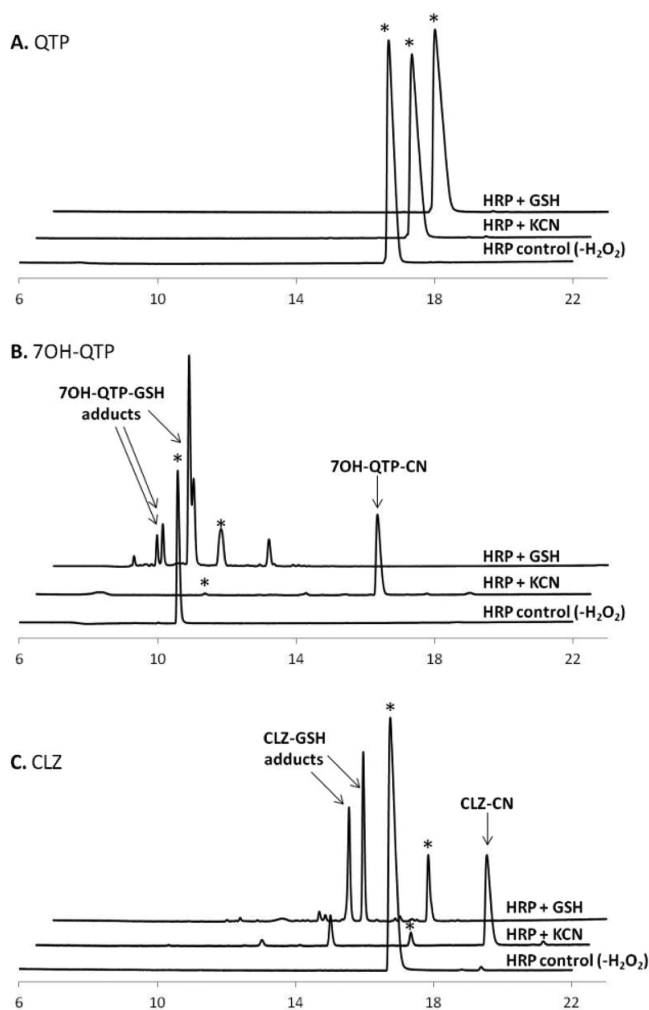


**Figure 6.** LC-UV chromatograms from HRP-catalyzed incubations with CLZ, QTP, and 7OH-QTP. Chromatograms ( $\lambda = 254$  nm) were obtained after 20 min incubations containing 20 U/mL HRP, 0.8 mM  $\text{H}_2\text{O}_2$ , and 20  $\mu\text{M}$  QTP, 7OH-QTP, or CLZ in 100  $\mu\text{M}$  phosphate buffer, pH 7.4. When indicated, incubations also contained 5 mM GSH or 4 mM KCN. The peak for the parent drug is indicated with an asterisk. The peak heights for the  $-\text{H}_2\text{O}_2$  controls for QTP, 7OH-QTP, and CLZ are 372, 520, and 307 mAU, respectively.

not observed in any of the incubations with dibenzothiazepin-11-one.

**Detection of 7OH-QTP Adducts in Rat.** Microsomal incubations do not simulate all of the available *in vivo* QTP clearance mechanisms. For this reason, we verified that similar GSH adducts were generated in rat microsomes and then proceeded to look for evidence of the bioactivation of QTP *in vivo*. The bile duct was cannulated in three 12 week old male Sprague–Dawley rats. Blank bile was collected immediately prior to oral dosing of 20 mg/kg QTP, and additional bile samples were collected 2 and 7 hours post-QTP dose. Both glutathione and mercapturic acid adducts of 7OH-QTP were detected from the 2 h postdose bile samples when evaluated by LC-MS/MS. Only mercapturic acid adducts were detected in the 7 h samples, nothing was detected for the predose bile samples, and no 7OH-QTP adducts were detected in plasma. The chromatogram and MS/MS spectrum of a representative adduct are shown in Figure 7 (spectra for all adducts are included in the Supporting Information).

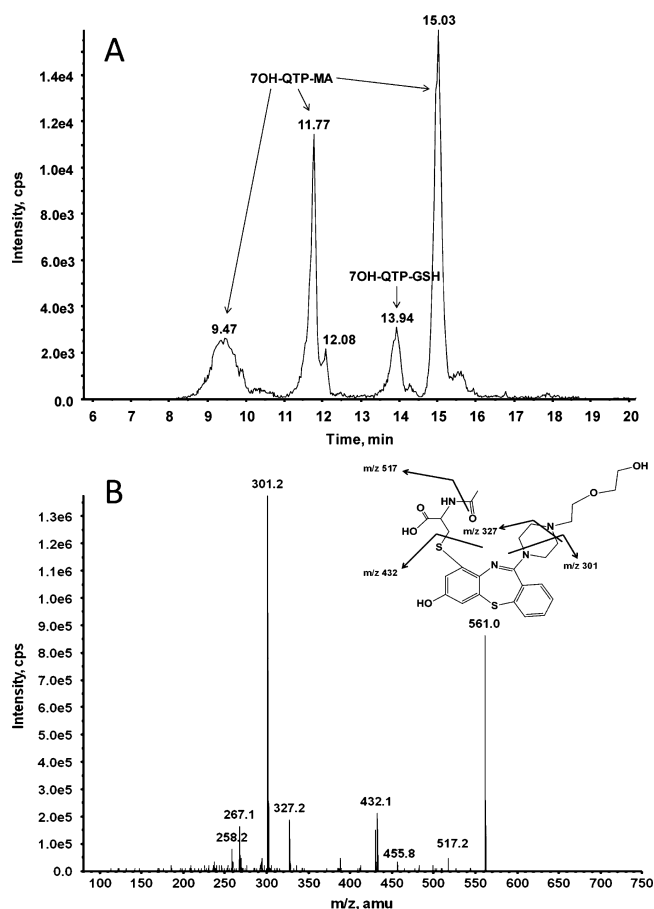


**Figure 7.** Detection of GSH and mercapturic acid adducts in bile after oral dosing of QTP. QTP was dosed by oral gavage (20 mg/kg) in bile duct-cannulated 12 week old male Sprague–Dawley rats. In panel A, the detected mercapturic acid adducts are labeled as 7OH-QTP-MA in the LC-MS/MS chromatogram obtained from bile collected 2 h postdose. The MS/MS spectrum and proposed molecular fragments for the peak at 11.77 min are shown in panel B. The masses displayed for the fragmentation of the piperazine correspond to the additional fragmentation of the thioether bond. Similar fragmentation patterns were observed for all three mercapturic acid adducts.

## DISCUSSION

The molecular design of QTP removed the bridging nitrogen, which had been implicated in the toxicity of CLZ. In the current report, we present evidence that QTP itself does not generate significant levels of the toxic nitrenium ion observed with CLZ. However, the hydroxylated QTP metabolite (7OH-QTP) was shown to form covalent adducts, and a mechanism has been proposed that involves the formation of a reactive quinone-imine, which readily reacts with nucleophiles such as free sulfhydryl groups. While we propose that the quinone-imine is the primary reactive metabolite generated, the continued formation of a nitrenium ion involving the piperazine cannot be ruled out based on the extensive cyanide adduct formation when 7OH-QTP was incubated with peroxidases. Additionally, the observed 7OH-QTP homodimers and NAT heterodimers support the formation of a 7OH-QTP free radical, which may condense with the cyanyl radical, offering an alternative mechanism for the formation of the cyanide adduct that does not require nitrenium formation. The toxicological implication of the 7OH-QTP radical is of unknown significance.

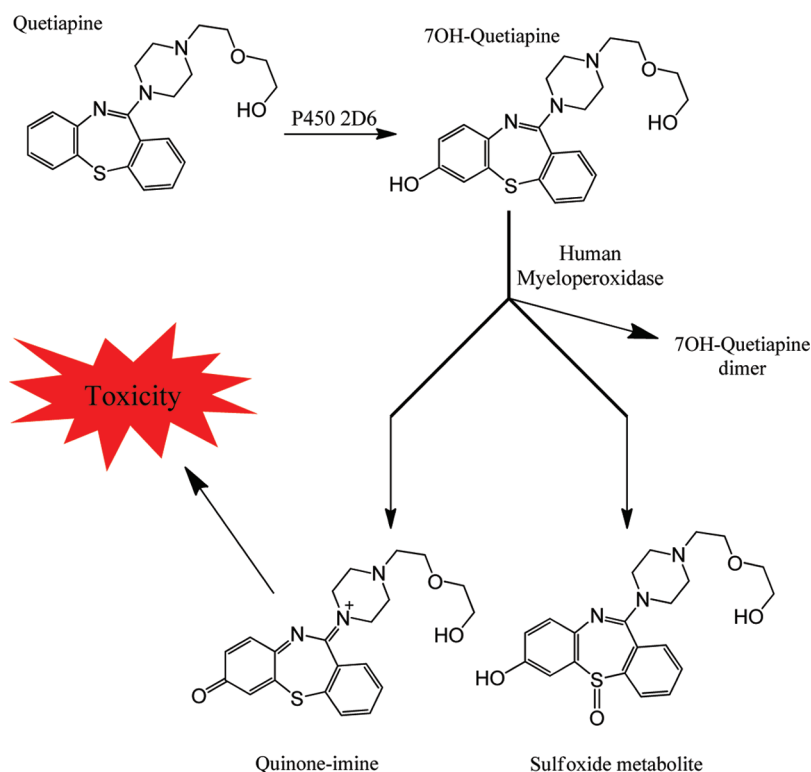


Figure 8. Proposed mechanism for QTP bioactivation.

While the formation of bioreactive and potentially toxic metabolites was not directly observed at meaningful levels during the incubation of QTP with peroxidases, reactive metabolites were trapped from QTP in hepatic microsomal incubations. The formation of reactive QTP intermediates appears to be primarily predicated on the initial conversion of QTP to 7OH-QTP and then further oxidation to form the electrophilic quinone-imine. The proposed bioactivation pathway is in Figure 8. These results are similar to those found with the CLZ analog fluperlapine and hydroxyfluperlapine.<sup>24</sup>

Clinically, the incidence of toxicity with QTP is much lower than for CLZ despite similar dosages for both drugs. This is likely due to two major factors. First, the nature of the reactive species being generated: the nitrenium ion (even with the positive charge of the CLZ nitrenium delocalized) is a harder electrophile than the quinone-imine formed by QTP as indicated by the cyanide trapping experiments for CLZ in the HRP experiments. Second, only the 7OH-QTP metabolite appears to be extensively bioactivated, and in QTP multiple-dose human pharmacokinetic studies,<sup>25</sup> the steady state ratio of 7OH-QTP:QTP is only about 10%. Oxidative damage and covalent modification of proteins should be decreased in QTP patients over those taking CLZ. An increased safety profile due to decreasing the reactive metabolite burden is similarly observed with the CLZ analogue olanzapine. Olanzapine has decreased patient toxicity despite forming the same reactive metabolites that CLZ forms presumably because it is more potent, which allows 10–20 times lower doses to be given to patients.<sup>26,27</sup>

Efforts were made to use physiologically relevant concentrations of QTP, and we believe 20  $\mu$ M reflects an anticipated hepatic QTP concentration achievable in a reasonable fraction of patients. QTP dosages administered vary widely depending on the treatment condition and patient response to the

medication, but a common range is 100–750 mg/day.<sup>28,29</sup> In multiple dose pharmacokinetic studies, 250 mg twice daily dosing resulted in a mean plasma  $C_{\max}$  of  $3 \pm 1$   $\mu$ M, and the liver to plasma ratio for QTP has been reported to be 3.5–8.7-fold.<sup>30,31</sup> Additionally, codosing with the CYP3A4 inhibitor ketoconazole increased QTP  $C_{\max}$  4-fold, and renal and hepatic impairment increased plasma QTP levels by approximately 2-fold.<sup>32</sup> CLZ tends to have higher plasma concentrations but lower liver to plasma ratios.<sup>33</sup> The 7OH-QTP concentration was matched to QTP and CLZ for clarity even though in vivo hepatic levels are unlikely to be 20  $\mu$ M.

In support of the in vivo relevance of the findings, the rat in vivo data showed that upon oral dosing of QTP, 7OH-QTP-GSH and corresponding mercapturic acid adducts were observed in rat bile. Typically, the enzymatic breakdown of GSH adducts to generate mercapturic acid adducts by  $\gamma$ -glutamyl transferase and cellular dipeptidases is thought to happen in the kidney, which would require export of the GSH adduct back into the blood.<sup>34</sup> We did not observe 7OH-QTP-GSH or -mercaptate adducts in the plasma. We do not believe that the 7OH-QTP-mercaptate adducts detected in rat bile necessarily require export of 7OH-QTP-GSH to the kidney. In the rat, expression levels of  $\gamma$ -glutamyl transferase and cellular dipeptidases in the bile duct are sufficient to facilitate the degradation of GSH adducts.<sup>35</sup>

Clinical toxicity related to QTP-induced neutropenia and hepatotoxicity is consistent with the presented findings. High MPO levels in activated macrophages predispose these cells to oxidative damage from 7OH-QTP through catalysis of the hydroquinone to the electrophilic quinone-imine. Liver damage would also be expected as generation of the reactive QTP metabolite can be catalyzed by hepatic P450.

The formation of 7OH-QTP is catalyzed by P450 2D6. P450 2D6 is genetically polymorphic with over 80 alleles identified

corresponding to four phenotypic categories: ultrarapid metabolizers (3–5%), extensive metabolizers (70–80%), intermediate metabolizers (10–15%), and poor metabolizers (7–10%).<sup>36–39</sup> It would be of interest to know if low 2D6 expression resulted in a protective effect due to lower levels of 7OH-QTP and a lower incidence of hepatic and white blood cell toxicities. Alternatively, would 2D6 high-expression individuals have increased levels of 7OH-QTP, and would this translate into increased toxicity risk?

In summary, we have demonstrated that through structural modification of CLZ, the second generation drug QTP has reduced the formation of reactive metabolites when directly reacted with peroxidases. However, a major QTP metabolite, 7OH-QTP, can react with peroxidases to generate a free radical and an electrophilic quinone-imine, which may explain the reduced yet still observed clinical toxicity.

## ■ ASSOCIATED CONTENT

### ■ Supporting Information

MS/MS spectra, figure, HPLC-UV chromatograms, and extracted ion chromatograms. This material is available free of charge via the Internet at <http://pubs.acs.org>.

## ■ AUTHOR INFORMATION

### Corresponding Author

\*E-mail: [cameron@scripps.edu](mailto:cameron@scripps.edu).

### Notes

The authors declare no competing financial interest.

## ■ ABBREVIATIONS

CLZ, clozapine; QTP, quetiapine; 7OH-QTP, 7-hydroxyquetiapine; MPO, myeloperoxidase; HRP, horseradish peroxidase; HLM, human liver microsome; MRM, multiple reaction monitoring; NAT, N-acetyltyrosine

## ■ REFERENCES

- (1) Lindenmayer, J. P., Brown, D., Liu, S., Brecher, M., and Meulien, D. (2008) The efficacy and tolerability of once-daily extended release quetiapine fumarate in hospitalized patients with acute schizophrenia: A 6-week randomized, double-blind, placebo-controlled study. *Psychopharmacol. Bull.* 41, 11–35.
- (2) Small, J. G., Hirsch, S. R., Arvanitis, L. A., Miller, B. G., and Link, C. G. (1997) Quetiapine in patients with schizophrenia. A high- and low-dose double-blind comparison with placebo. Seroquel Study Group. *Arch. Gen. Psychiatry* 54, 549–557.
- (3) Bowden, C. L., Grunze, H., Mullen, J., Brecher, M., Paulsson, B., Jones, M., Vagero, M., and Svensson, K. (2005) A randomized, double-blind, placebo-controlled efficacy and safety study of quetiapine or lithium as monotherapy for mania in bipolar disorder. *J. Clin. Psychiatry* 66, 111–121.
- (4) Vieta, E., Mullen, J., Brecher, M., Paulsson, B., and Jones, M. (2005) Quetiapine monotherapy for mania associated with bipolar disorder: Combined analysis of two international, double-blind, randomised, placebo-controlled studies. *Curr. Med. Res. Opin.* 21, 923–934.
- (5) Uetrecht, J., Zahid, N., Tehim, A., Fu, J. M., and Rakhit, S. (1997) Structural features associated with reactive metabolite formation in clozapine analogues. *Chem.-Biol. Interact.* 104, 117–129.
- (6) Uetrecht, J. P. (1992) Metabolism of clozapine by neutrophils. Possible implications for clozapine-induced agranulocytosis. *Drug Saf.* 7 (Suppl. 1), 51–56.
- (7) Chandrasekaran, P. K. (2008) Agranulocytosis monitoring with Clozapine patients: To follow guidelines or to attempt therapeutic controversies? *Singapore Med. J.* 49, 96–99.

- (8) Kalgutkar, A. S., and Didiuk, M. T. (2009) Structural alerts, reactive metabolites, and protein covalent binding: how reliable are these attributes as predictors of drug toxicity? *Chem. Biodiversity* 6, 2115–2137.

- (9) Cowan, C., and Oakley, C. (2007) Leukopenia and neutropenia induced by quetiapine. *Prog. Neuro-Psychopharmacol. Biol. Psychiatry* 31, 292–294.

- (10) Croarkin, P., and Rayner, T. (2001) Acute neutropenia in a patient treated with quetiapine. *Psychosomatics* 42, 368.

- (11) Ruhe, H. G., Becker, H. E., Jessurun, P., Marees, C. H., Heeringa, M., and Vermeulen, H. D. (2001) Agranulocytosis and granulocytopenia associated with quetiapine. *Acta Psychiatr. Scand.* 104, 311–313; discussion 313–314.

- (12) Shankar, B. R. (2007) Quetiapine-induced leucopenia and thrombocytopenia. *Psychosomatics* 48, 530–531.

- (13) Atasoy, N., Erdogan, A., Yalug, I., Ozturk, U., Konuk, N., Atik, L., and Ustundag, Y. (2007) A review of liver function tests during treatment with atypical antipsychotic drugs: a chart review study. *Prog. Neuro-Psychopharmacol. Biol. Psychiatry* 31, 1255–1260.

- (14) El Hajj, I., Sharara, A. I., and Rockey, D. C. (2004) Subfulminant liver failure associated with quetiapine. *Eur. J. Gastroenterol. Hepatol.* 16, 1415–1418.

- (15) Naharci, M. I., Karadurmus, N., Demir, O., Bozoglu, E., Ak, M., and Doruk, H. (2011) Fatal hepatotoxicity in an elderly patient receiving low-dose quetiapine. *Am. J. Psychiatry* 168, 212–213.

- (16) Shpaner, A., Li, W., Ankoma-Sey, V., and Botero, R. C. (2008) Drug-induced liver injury: Hepatotoxicity of quetiapine revisited. *Eur. J. Gastroenterol. Hepatol.* 20, 1106–1109.

- (17) Bakken, G. V., Rudberg, I., Christensen, H., Molden, E., Refsum, H., and Hermann, M. (2009) Metabolism of quetiapine by CYP3A4 and CYP3A5 in presence or absence of cytochrome B5. *Drug Metab. Dispos.* 37, 254–258.

- (18) Grimm, S. W., Richtand, N. M., Winter, H. R., Stams, K. R., and Reece, S. B. (2006) Effects of cytochrome P450 3A modulators ketoconazole and carbamazepine on quetiapine pharmacokinetics. *Br. J. Clin. Pharmacol.* 61, 58–69.

- (19) Hasselstrom, J., and Linnet, K. (2006) In vitro studies on quetiapine metabolism using the substrate depletion approach with focus on drug-drug interactions. *Drug Metab. Drug Interact.* 21, 187–211.

- (20) Lu, W., and Uetrecht, J. P. (2008) Peroxidase-mediated bioactivation of hydroxylated metabolites of carbamazepine and phenytoin. *Drug Metab. Dispos.* 36, 1624–1636.

- (21) Moreno, S. N., Stolze, K., Janzen, E. G., and Mason, R. P. (1988) Oxidation of cyanide to the cyanyl radical by peroxidase/H<sub>2</sub>O<sub>2</sub> systems as determined by spin trapping. *Arch. Biochem. Biophys.* 265, 267–271.

- (22) Chen, Y. R., Deterding, L. J., Tomer, K. B., and Mason, R. P. (2000) Nature of the inhibition of horseradish peroxidase and mitochondrial cytochrome c oxidase by cyanyl radical. *Biochemistry* 39, 4415–4422.

- (23) Malencik, D. A., Sprouse, J. F., Swanson, C. A., and Anderson, S. R. (1996) Dityrosine: Preparation, isolation, and analysis. *Anal. Biochem.* 242, 202–213.

- (24) Lai, W. G., Gardner, I., Zahid, N., and Uetrecht, J. P. (2000) Bioactivation and covalent binding of hydroxyfluperlapine in human neutrophils: Implications for fluperlapine-induced agranulocytosis. *Drug Metab. Dispos.* 28, 255–263.

- (25) Li, K. Y., Li, X., Cheng, Z. N., Peng, W. X., Zhang, B. K., and Li, H. D. (2004) Multiple dose pharmacokinetics of quetiapine and some of its metabolites in Chinese suffering from schizophrenia. *Acta Pharmacol. Sin.* 25, 390–394.

- (26) Gardner, I., Zahid, N., MacCrimmon, D., and Uetrecht, J. P. (1998) A comparison of the oxidation of clozapine and olanzapine to reactive metabolites and the toxicity of these metabolites to human leukocytes. *Mol. Pharmacol.* 53, 991–998.

- (27) Gardner, I., Leeder, J. S., Chin, T., Zahid, N., and Uetrecht, J. P. (1998) A comparison of the covalent binding of clozapine and



olanzapine to human neutrophils in vitro and in vivo. *Mol. Pharmacol.* 53, 999–1008.

(28) McConville, B. J., Arvanitis, L. A., Thyrum, P. T., Yeh, C., Wilkinson, L. A., Chaney, R. O., Foster, K. D., Sorter, M. T., Friedman, L. M., Brown, K. L., and Heubi, J. E. (2000) Pharmacokinetics, tolerability, and clinical effectiveness of quetiapine fumarate: An open-label trial in adolescents with psychotic disorders. *J. Clin. Psychiatry* 61, 252–260.

(29) DeVane, C. L., and Nemeroff, C. B. (2001) Clinical pharmacokinetics of quetiapine: an atypical antipsychotic. *Clin. Pharmacokinet.* 40, 509–522.

(30) Hopenwasser, J., Mozayani, A., Danielson, T. J., Harbin, J., Narula, H. S., Posey, D. H., Shrode, P. W., Wilson, S. K., Li, R., and Sanchez, L. A. (2004) Postmortem distribution of the novel antipsychotic drug quetiapine. *J. Anal. Toxicol.* 28, 264–267.

(31) Wang, J. S., Zhu, H. J., Markowitz, J. S., Donovan, J. L., and DeVane, C. L. (2006) Evaluation of antipsychotic drugs as inhibitors of multidrug resistance transporter P-glycoprotein. *Psychopharmacology (Berlin, Ger.)* 187, 415–423.

(32) Thyrum, P. T., Wong, Y. W., and Yeh, C. (2000) Single-dose pharmacokinetics of quetiapine in subjects with renal or hepatic impairment. *Prog. Neuro-Psychopharmacol. Biol. Psychiatry* 24, 521–533.

(33) Manjunath, K., and Venkateswarlu, V. (2005) Pharmacokinetics, tissue distribution and bioavailability of clozapine solid lipid nanoparticles after intravenous and intraduodenal administration. *J. Controlled Release* 107, 215–228.

(34) Hinchman, C. A., and Ballatori, N. (1994) Glutathione conjugation and conversion to mercapturic acids can occur as an intrahepatic process. *J. Toxicol. Environ. Health* 41, 387–409.

(35) Hinchman, C. A., Matsumoto, H., Simmons, T. W., and Ballatori, N. (1991) Intrahepatic conversion of a glutathione conjugate to its mercapturic acid. Metabolism of 1-chloro-2,4-dinitrobenzene in isolated perfused rat and guinea pig livers. *J. Biol. Chem.* 266, 22179–22185.

(36) Kirchheiner, J., Henckel, H. B., Meineke, I., Roots, I., and Brockmoller, J. (2004) Impact of the CYP2D6 ultrarapid metabolizer genotype on mirtazapine pharmacokinetics and adverse events in healthy volunteers. *J. Clin. Psychopharmacol.* 24, 647–652.

(37) Bertilsson, L., Dahl, M. L., Dalen, P., and Al-Shurbaji, A. (2002) Molecular genetics of CYP2D6: Clinical relevance with focus on psychotropic drugs. *Br. J. Clin. Pharmacol.* 53, 111–122.

(38) De Gregori, M., Allegri, M., De Gregori, S., Garbin, G., Tinelli, C., Regazzi, M., Govoni, S., and Ranzani, G. N. (2010) How and why to screen for CYP2D6 interindividual variability in patients under pharmacological treatments. *Curr. Drug Metab.* 11, 276–282.

(39) Rebsamen, M. C., Desmeules, J., Daali, Y., Chiappe, A., Diemand, A., Rey, C., Chabert, J., Dayer, P., Hochstrasser, D., and Rossier, M. F. (2009) The AmpliChip CYP450 test: Cytochrome P450 2D6 genotype assessment and phenotype prediction. *Pharmacogenomics J.* 9, 34–41.